Derived Performance Metrics and Angular Efficiency of an Ionic Liquid Ferrofluid Electrospray Propulsion Concept

Brandon A. Jackson,[1] Kurt J. Terhune[2] and Lyon B. King[3]
Michigan Technological University, Houghton, MI, 49931, USA

The performance of a single tip ionic liquid ferrofluid electrospray source was estimated. The electrospray source was sprayed until the fluid reservoir was depleted (typically 15 to 18 hours) with a magnetic field strength ranging from 320 to 500 G. While emitting, the angular divergence of the spray was measured, which yielded an average angular power efficiency of 94%. The mass-flow rate was also approximate via timelapse imagery taken of the fluid meniscus allowing propulsion parameters to be derived. It was found the mass flow rate of the source averaged 25 ng/s, with a specific impulse of 1385 s and a thrust per emitter of 0.380 µN.

I. Introduction

IN 2013, Meyer and King reported on a new type of electrospray which combines a magneto-electric instability to achieve electrospray emission.[1, 2] The novel fluid utilized in their research is an ionic liquid ferrofluid (ILFF), which consists of an ionic liquid (IL) carrier fluid with nanoscale magnetic particles suspended in the fluid in such a manner that they will neither settle nor clump together.[3] The combined fluid maintains the desirable properties of the carrier IL (low vapor pressure, high electrical conductivity) while becoming super paramagnetic.

In the presence of a sufficiently strong magnetic field, the surface of a ferrofluid will deform into an array of peaks, known as a normal-field instability. When an electric field is applied, electric stresses will develop, further stressing the instability – enabling electrospray emission to be achieved. For sessile drops or confined volumes of ferrofluid, an isolated peak can be formed and studied.

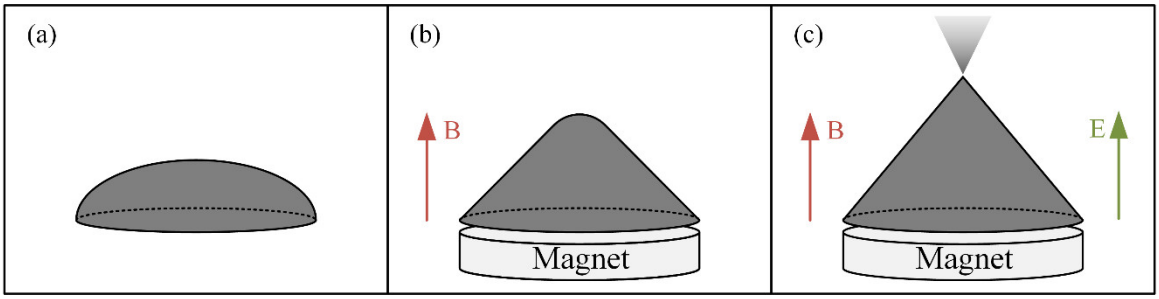

Figure 1: Electrospray emission from a combined ferro-electrohyrodynamic instability: (a) In the absence of an applied field, a sessile drop of ILFF spreads. (b) The application of a magnetic field stresses the fluid interface resulting in the fluid rising into a peak. (c) Finally, the addition of a strong electric field further stresses the fluid interface until emission onset.

The unique ability of ferrofluids to self-assemble into pattern of peaks and emit has interesting potential for electrospray propulsion – providing an alternative solution to MEMS fabricated emitters or capillary needles. In recent years, several authors have published on this novel form of electrospray. Terhune performed time-of-flight measurements on both an ILFF normal field instability and a capillary needle source.[4, 5] Jackson et. al presented a computational tool to predict the meniscus geometry and analyze surface stresses of the combined magneto-electric

[1] Ph.D. Candidate, Mechanical Engineering – Engineering Mechanics, Email: bajackso@mtu.edu
[2] Ph.D. Candidate, Mechanical Engineering – Engineering Mechanics, Email: kjterhun@mtu.edu
[3] Ron and Elaine Starr Professor in Space Systems, Mechanical Engineering – Engineering Mechanics Email: lbking@mtu.edu

instability for a single peak prior to onset of emission.[6] In 2017, Jackson also reported previous work which demonstrated long duration emission of an ILFF electrospray source.[7]

Since electrospray emission from a magneto-electric instability was only recently demonstrated, many fundamental questions regarding the emission behavior remain to be researched. Two of these questions are: (1) what is angular divergence of spray from a normal-field instability, and (2) can this source of electrospray provide desirable performance for spacecraft propulsion.

An effective way to quantify the angular divergence of an electrospray source is through the angular power efficiency factor, η_θ. This factor accounts for the reduction in overall power efficiency which results power carried by particles with off-axis velocity components. This factor accounts for the power lost by particles with off-axis velocity components and causes a reduction in the overall power efficiency of a thruster. The power efficiency, i.e. the efficiency at which electric power is converted

$$\eta_T = \frac{T^2}{2\dot{m}P_{in}} \tag{1}$$

in which η_T is the power efficiency, T is the resultant thrust, $\dot{m}$ is the propellant mass flow rate, P_{in} is the electrical power supplied. For an electrospray thruster, the power efficiency can be approximated in terms of individual inefficiencies in the following expression presented by Lozano:[8]

$$\eta_T = \eta_i \eta_{tr}^2 \eta_\theta \eta_E \eta_P \tag{2}$$

The first two undefined terms on the right-hand side of Eq (2)are the ionization and transmission efficiencies, η_i and η_{tr}, respectively. They account for...accelerator. inefficiencies in ionizing all of the available propellant and intercepted current by the extractor or accelerator. The angular power efficiency is expressed as η_θ. The fourth term is the energy efficiency, η_E, which is the energy efficiency, which accounts for the inefficiencies resulting from not accelerating a particle to the full extraction potential. Finally, η_P is the polydispersive efficiency, which accounts for energy wasted accelerating particles of different charge-to-mass ratios. Note: Eq. (2) makes the assumption that the efficiency factors are completely decoupled and that there is, for example, no angular dependence in the polydispersive efficiency. In practice, some terms are observed to have angular dependence; however, this model serves as a concise statement of various factors impacting efficiency. With this simplification, the angular power efficiency factor simply becomes:

$$\eta_\theta = \left(\frac{\text{Thrust w/ ang. dep.}}{\text{Thrust w/o ang. dep.}} \right)^2 = \left(\int_0^{\theta_{\max}} \rho_I(\theta) \sin\theta \cos\theta d\theta \Big/ \int_0^{\theta_{\max}} \rho_I(\theta) \sin\theta d\theta \right)^2 \tag{3}$$

where $\rho_I(\theta)$ is the angular current density distribution function. Evaluating this expression provides a concise term which can be used to quantify the angular divergence and correlate influential factors—such as mass flow rate and emission current.

The second objective of this study was to estimate the propulsion performance of parameters for an ILFF electrospray source. To serve as a viable propulsion technology, a thruster emitting from the combined magneto-electric instability will need to achieve a performance levels comparable to competing technologies. Ideally, propulsion performance would be measured through direct measurement of produced thrust – a challenging endeavor given the thrust produced by a single electrospray emitter. For this study, preliminary performance metrics will be derived from emission current, mass-flow rate, and extraction voltage.

II. Description of Apparatus and Test Facility

All experiments were performed in the Ion Space Propulsion laboratory at Michigan Technological University. The electrospray emitter apparatus utilized for this study was designed by Terhune[4] with modifications in the manner in which the extractor and collector electrodes were mounted. A diagram of the emitter apparatus is presented in Figure 2.

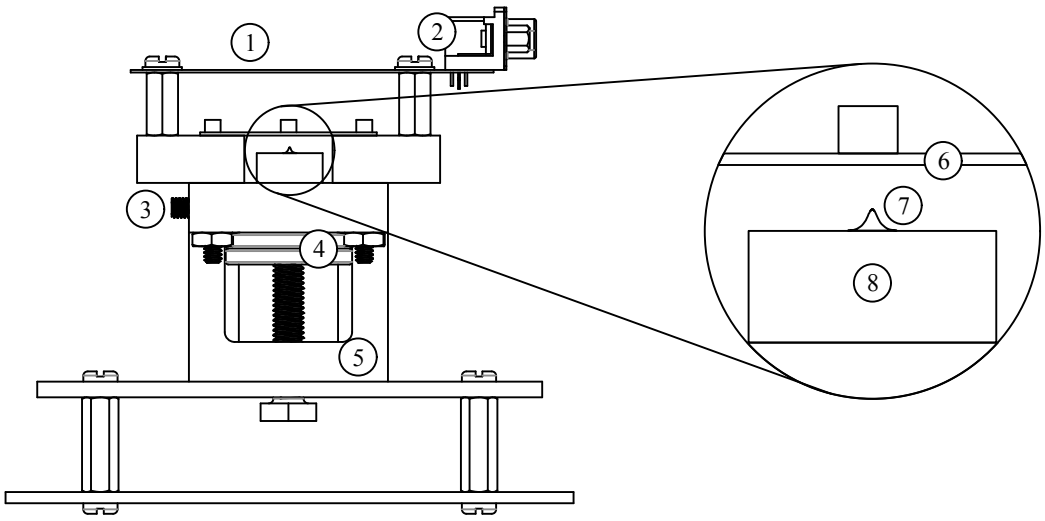

Figure 2: Electrospray emission apparatus. (1) Current collector, (2) DB-9 surface mount connector, (3) electrical bias terminal, (4), N-52 magnets, (5) PTFE isolation block, (6) Extractor electrode, (7) ferrofluid instability, and (8) fluid reservoir.

The extractor electrode was positioned 2.85 mm downstream of the fluid reservoir and positioned using Teflon alignment pins. The extractor and current collector were separated by 15.40 mm with an extractor thickness of 1.13 mm. The fluid reservoir was biased, and the extraction electrode was grounded.

Emission current was measured using a segmented Faraday probe consisting of nine concentric rings which was fabricated from a copper-clad PCB (see Figure 3). Current on each probe was measured simultaneously using nine EEVBlog μCurrent meters set to a resolution of 10 mV/nA and full-scale range of 1200 nA. Segmenting the Faraday probe enabled the emission current distribution to be resolved – permitting the calculation of an angular power efficiency factor, η_θ, for the emitter.

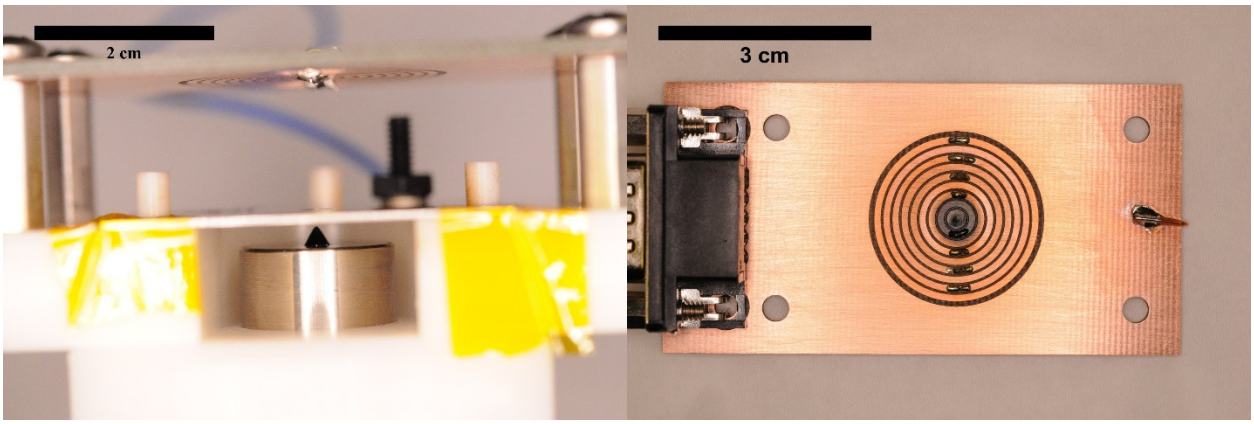

Figure 3: (Left) Frontal view of the assembled ILFF electrospray emission apparatus. (Right) Current collector after approximately 15 hours of emission. Ferrofluid buildup can be observed on the center rings with decreasing intensity as the radial distance increases. Continuity between adjacent pads was measured after testing to detect pad-to-pad shorts. None were ever detected.

Testing was performed at vacuum within the Micropropulsion Facility-2 within the Ion Space Propulsion Laboratory at Michigan Technological University. This facility is approximately a 60-liter cylinder and is roughed down using a 300 liter/min tri-scroll pump and a 280 liter/second turbomolecular pump. The base pressure of this facility is approximately 4×10^{-7} torr. Emission was conducted only after the tank pressure reached approximately 1×10^{-6} torr. A single emitter was found to have no measurable impact on tank pressure and tank pressure was observed to drop continuously during testing until the base pressure was obtained.

The ferrofluid utilized for this investigation has an Emim-NTf2 carrier fluid with polymer-stabilized 10-12 nm diameter magnetic particles. The ILFF was produced by the *Key Centre for Polymers and Colloids* at the University of Sydney. The fluid has a density of 1815 kg/m^3, a conductivity of 0.63 S/m, and a surface tension of 32.4 mN/m.[3, 9-11]

III.Experimental Methods

The reservoir was infused with 14-µL of ferrofluid, in the presence of a magnetic field, using a 50-µL syringe and syringe pump. Fluid was infused into the reservoir at a flow rate of 1-µL/s. Due to uncertainty in the amount of fluid delivered, actual volume of the peak was estimated by performing a volume integral on an image of the peak using the extractor diameter as a reference dimension. The fluid was then allowed to sit at vacuum (~1 torr) for at least 2 hours prior to being sprayed. The ferrofluid reservoir could not be replenished during emission, so the length of studies was limited by the volume of fluid in the reservoir.

The fluid reservoir was biased using a ±5kV Ultravolt HVA precision high bandwidth power supply set to output a 500 mHz square wave yielding positive and negative extraction voltages of equal magnitude. During the start-up phase electrospray source, the fluid peak was structure was very sensitive and the extraction potential was frequently adjusted to maintain emission. Emission from the fluid peak would then stabilize into a constant voltage mode after 45 to 180 minutes of operation. The constant voltage mode of emission could be sustained for an excess of 10 hours without adjusting the extraction potential. Once emission self-extinguished, the extraction potential was increased to restart emission, which would last 10s of seconds to minutes. Each time the source extinguished, the extraction potential would be increased to restart emission until the fluid in the reservoir depleted or the maximum range of the voltage of the power supply was reached. The fluid profile at select intervals showing typical emission behavior is presented in Figure 4. A typical emission telemetry is presented in Figure 5.

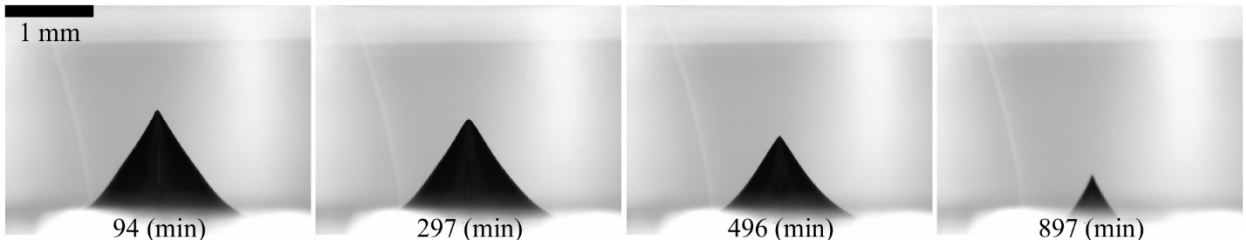

Figure 4: Ferrofluid interface during select moment of constant voltage emission test. Extraction voltage was held constant between 80 and 680 minutes.

Mass-flow rates of the single tip ILFF emitter were estimated by analyzing time-lapse imagery of the peak during emission. Images of the emitter were taken at 30-second interval using an OptixCam Summit K2 5.1 MP USB camera attached to a stereo microscope. Edge detection and integration of the peak profile enabled the instantaneous fluid volume to be approximated. The volume-time relationship was fit with a smoothing spline and differentiated to obtain mass-flow rate. Approximate values of average mass-to-charge ratio, velocity, specific impulse, and thrust were obtained using the average mass-flow rate, emission current, and emission potential during the constant voltage portion of the emission telemetry.

Three emission studies were conducted using a 321, 388, and 495 gauss magnetic field (measured at the top surface of the fluid reservoir). On average, emission was maintained for 17 hours for each run. The results of these tests are presented in the following two sections.

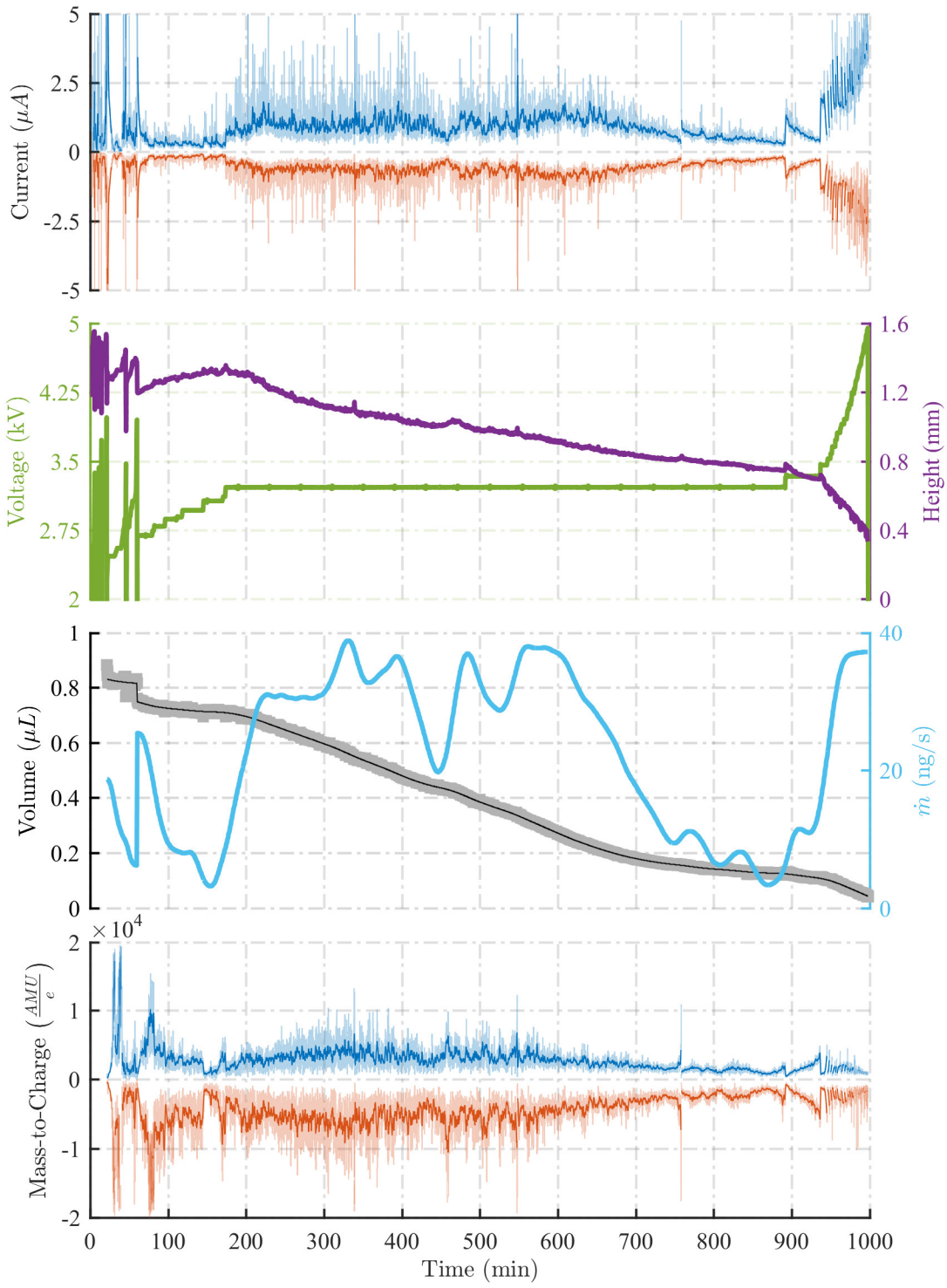

Figure 5: Telemetry for an entire electrospray emission test. 30 second moving average is overlayed. (B = 495 G)

IV. Angular Power Efficiency Factor

The segmented current collector, introduced in Section 2, permitted the angular current distribution to be measured within the emission plume during the entire duration of the emission telemetry. From the centroid position and area of each probe, the angular current density distribution function, $\rho_I(\theta)$, was obtained by fitting a PCHIP[4] curve to the angular current distribution. A sample Faraday trace obtained from the segmented probes as well as a current density distribution is shown in Figure 6.

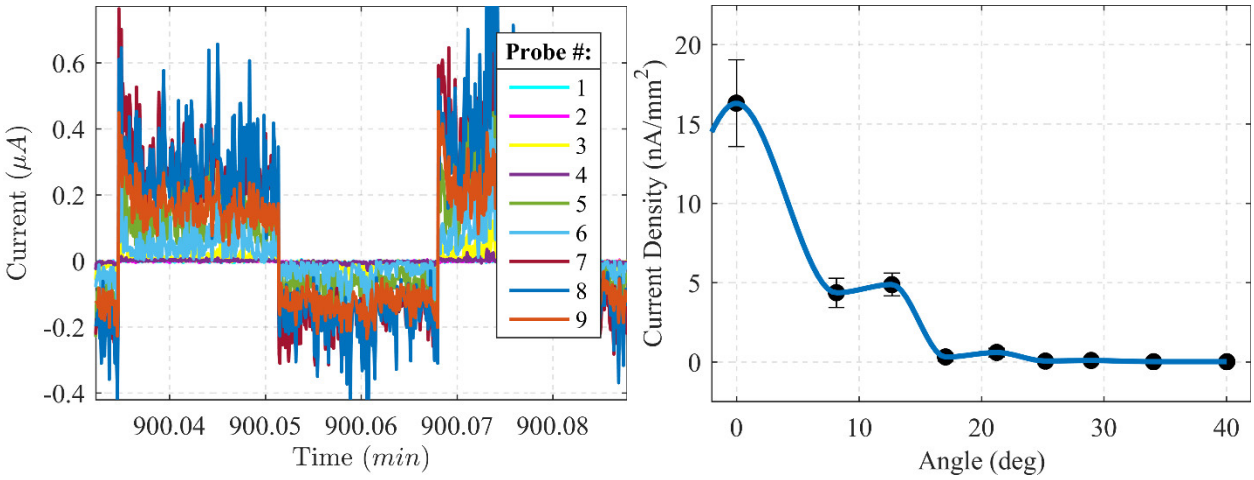

Figure 6: (Left) Typical Faraday trace obtained by simultaneously measuring current on all nine collectors. Probes are numbered sequentially, 9 being the inner most. (Right) Angular current density with fit.

The current density distribution was integrated using Eq. (3) and averaged over a 1-minute period to obtain the averaged angular power efficiency factor. The angular efficiencies for both polarities for the telemetry shown in Figure 5 are presented below at 25 minute intervals in Figure 7. The average efficiency measured for tests conducted using three different magnetic field strengths are presented in Table 1:

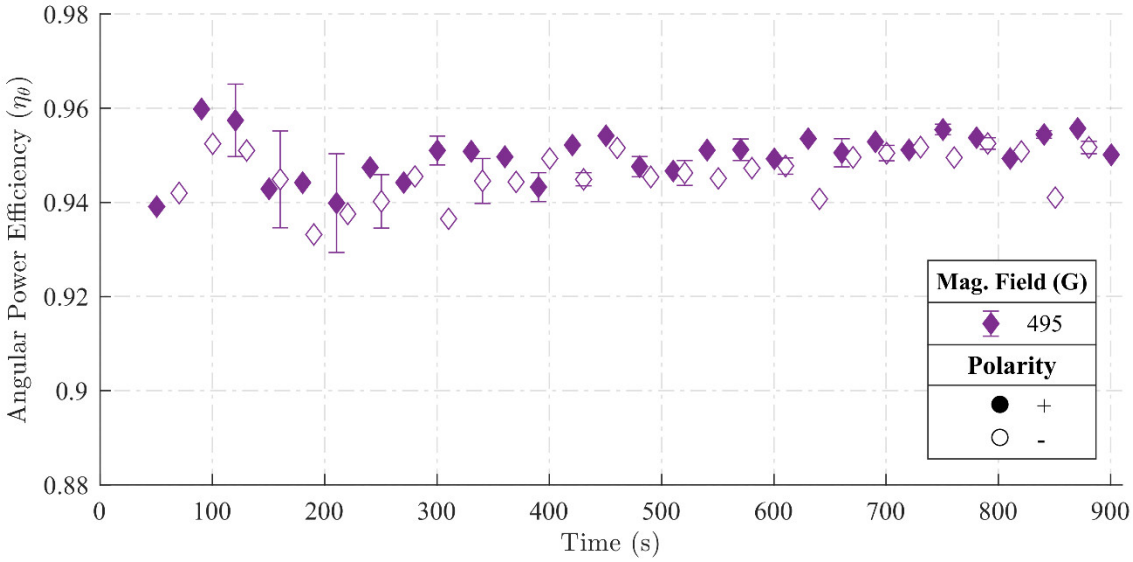

Figure 7: Angular power efficiency factor for both positive and negative emission polarities during a 17-hour emission study.

[4] Piecewise Cubic Hermite Interpolating Polynomial

Table 1: Tabulated comparison of angular power efficiency. Only angular efficiencies after 200 minutes were included in the averaging since prior to that time, not all sample sets were in the constant voltage operation mode.

Mag. Field (G)	Mean η_θ
321	0.9463 ± 0.0065
388	0.9365 ± 0.0068
495	0.9470 ± 0.0047

It can be observed that the angular efficiency for the negative polarity was consistently lower than that of the positive polarity. This observation was confirmed with a two-sample t-test, yielding $<10^{-5}$. This trend remained for emission studies conducted with a 321 and 388 gauss magnetic field. It was found that on average, a percent difference of 0.75% was present between the two polarities.

A difference in beam divergence of positive and negative polarity can be reasonably expected under the well-accepted premise that beam composition depends on polarity and that the composition of the beam has a significant influence on the divergence of the beam. Chiu et al.[12] performed a very comprehensive study using an externally wetted electrospray source emitting EMIM-NTf2, the same ionic liquid which serves as a carrier fluid for the ferrofluid studied herein. In their work, emission current and mass flow rate were measured with respect to emitter angle, which yielded distributions which are dependent on the current polarity. Their work also demonstrated that the beam composition depended strongly on polarity as well as angle by measuring the source using a quadrupole mass filter. In a comprehensive analysis of the 480 emitter iEPS thruster, Krejci et al. observed a much larger polarity dependence in angular efficiency of 0.801 and 0.828 for the positive and negative polarities, respectively.[13]

Moderate changes in emission current were observed to occur during emission without changing the extraction potential. This trend can be observed in Figure 5. When angular efficiency is plotted against emission current, which is presented in Figure 8, a noticeable trend develops between increasing emission current and decreasing angular efficiency. A correlation analysis was using the Spearman technique, yielding P-values which strongly confirm the correlation. The trend of reduced efficiency at higher emission currents is small and relatively insignificant. However, the influence of emission current on other efficiency factors remains unknown.

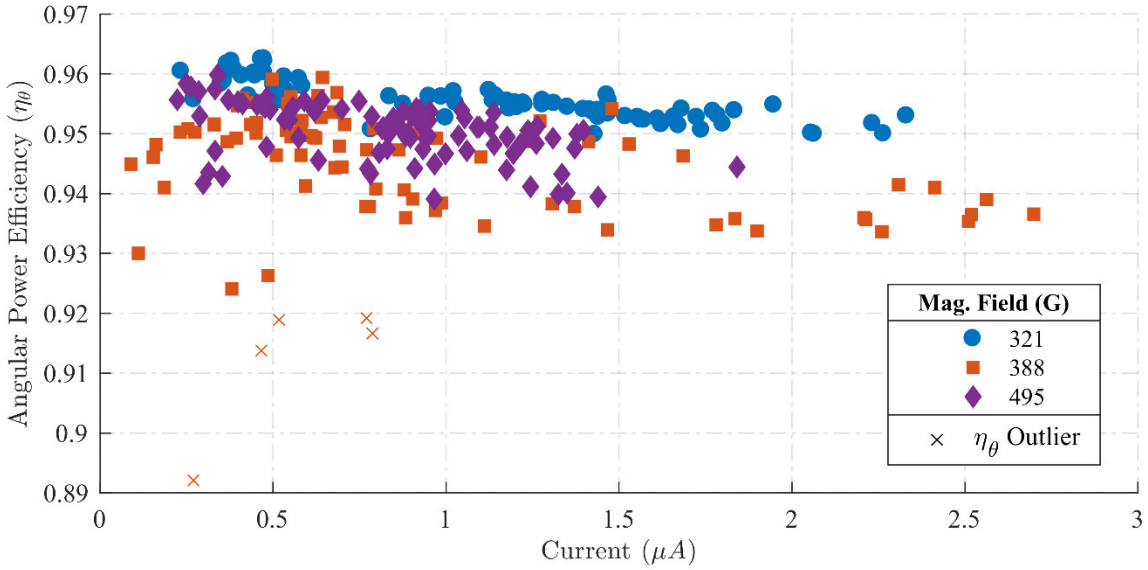

Figure 8: Angular efficiency and emission current correlation. Plotted points are taken from within the constant voltage portion of the emission telemetry. Outliers were detected using a using a median absolute deviation technique. A small trend can be observed between increasing emission current and reduced angular efficiency.

Table 2: Tabulated correlation coefficient for emission current angular efficiency relation

	B Field (G)		η_θ	Population (n)
I	321	R	-0.829	83
		P	0	
	388	R	-0.457	80
		P	2.47×10^{-5}	
	495	R	-0.506	85
		P	1.15×10^{-6}	

Previous researchers have observed a similar trend in angular efficiency and emission current while studying other electrospray sources operating via traditional mechanisms. While researching capillary needle emitters, Gamero-Castaño observed a broadening of the emission plume with an increase in emission current when emitting both EMIM-NTf2[14] as well as with propylene carbonate doped with an ionic liquid.[15] This broadening observed was attributed to an increase in satellite droplet formation. Gamero-Castaño also observed an increased production of higher mass-to-charge droplets at propellant flow rate.[14] Since particle of different mass-to-charge ratios respond differently to acceleration forces in the apex region, charge-to-mass ratios of the emitted species are accepted to be an influential factor in beam divergence.

V. Derived Propulsion Performance Parameters

From the three emission studies conducted for this research, propulsion performance parameters were derived. These metrics, presented in Table 3, include mass-low rate, specific impulse, and thrust-per emitter. Since thrust could not be measured directly, these parameters were approximated using the average mass-to-charge ratio of the emitted fluid. Performance parameters were calculated only during the constant voltage phase of the emission telemetry. First, the average emission current for both polarities was calculated as follows:

$$\bar{I}^{+,-} = \frac{1}{t_2 - t_1}\int_{t_1}^{t_2} I^{+,-} dt \tag{4}$$

The net average emission current becomes:

$$\bar{I} = \frac{1}{2}\left(\bar{I}^{+} + \bar{I}^{-}\right) \tag{5}$$

The average combined mass flow rate of the emitter is:

$$\dot{\bar{m}} = \frac{1}{t_2 - t_1}\int_{t_1}^{t_2} \dot{m} dt \tag{6}$$

where t_1 and t_2 are the start and end times of the constant voltage phase of emission. Finally, the average mass-to charge ratio was defined as:

$$m/q = \frac{\dot{\bar{m}}}{\bar{I}} \tag{7}$$

The velocity was then calculated using the average mass-to-charge ratio using Eq. (7). Thrust and specific impulse were calculated in terms of velocity.

$$v_e = \sqrt{\frac{2qV}{m}} \tag{8}$$

Table 3: Tabulated Derived Propulsion Metrics for Long Duration Emission tests. Average values calculated during constant voltage mode of emission.

		Test #		
		1	2	3
Magnetic Field (G)		495	321	388
Emission Duration (hr)		16.7	15.6	18.4
Average	Mass Flow Rate (ng/s)	24.8	32.8	26.6
	Emission Current (μA)	0.75	0.79	0.84
	Mass-to-Charge (kg/C)	3.31×10^{-5}	4.16×10^{-5}	3.61×10^{-5}
	Exhaust Velocity (m/s)	1.39×10^{4}	1.25×10^{4}	1.43×10^{4}
	Specific Impulse (s)	1422	1278	1455
	Thrust (μN)	0.346	0.412	0.380

The propulsion performance metrics between the three tests conducted were rather consistent. The specific impulse averaged 1385, producing an average thrust per emitter of 0.38 μN. However, the methodology utilized herein to estimate propulsion metrics is an over estimate of real performance. This approach assumes that all particles are accelerated to the full extraction potential. It is also assumed that a single value can accurately describe the mass-to-charge ratio. In the mixed ion-droplet regime,[5, 16, 17] which is operation mode of this emitter, the mass-to-charge ratio distribution spans several orders of magnitude. Future research into quantify the thrust produced by a ferrofluid electrospray emitter will incorporate mass spectrometry techniques to achieve more direct estimates of the mass-to-charge ratio and propulsion metrics.

VI. Conclusion

The long duration emission behavior of a novel form of electrospray which operates via a combined magneto-electric instability was studied. It was found that the emitter was capable of operation for durations in excess of 18 hours, limited only by the fluid volume contained in the emitter. During operation, the flow rate of the emitter averaged 28 ng/s (15.5 pL/s). The angular divergence of the emission current was measured and the emitter was found to have an angular propulsion efficiency factor of 94%. Propulsion performance metrics were derived for the thruster. These metrics lend credence to the concept of this type of electrospray and findings presented herein serve to justifies further efforts to refine the technology.

VII. References

1. Meyer IV, E. J., and King, L. B. "Electrospray from an Ionic Liquid Ferrofluid utilizing the Rosensweig Instability." 49th AIAA/ASME/SAE/ASEE Joint Propulsion Conferene & Exhibit, Paper No. AIAA-2013-3823, 14-17 July 2013, San Jose, CA, 2013.
2. IV, E. J. M., King, L. B., Jain, N., and Hawkett, B. S. "Ionic liquid ferrofluid electrospray with EMIM-NTf2 and ferrofluid mode studies with FerroTec EFH-1 in a non-uniform magnetic field," 2013.
3. King, L. B., Meyer, E., Hopkins, M. A., Hawkett, B. S., and Jain, N. "Self-Assembling Array of Magnetoelectrostatic Jets from the Surface of a Superparamagnetic Ionic Liquid," *Langmuir* Vol. 30, No. 47, 2014, pp. 14143-14150.
4. Terhune, K. J., King, L. B., Prince, B. D., Jain, N., and Hawkett, B. S. "Species measurements in the beam of an ionic liquid ferrofluid capillary electrospray source under magnetic stress," *52nd AIAA/SAE/ASEE Joint Propulsion Conference*. 2016, p. 4550.
5. Terhune, K. J., King, L. B., Hause, M. L., Prince, B. D., Jain, N., and Hawkett, B. S. "Species measurements in the beam of an ionic liquid ferrofluid electrospray source," *50th AIAA/ASME/SAE/ASEE Joint Propulsion Conference & Exhibit*. AIAA, Cleveland, OH, 2014.
6. Jackson, B. A., Terhune, K. J., and King, L. B. "Ionic liquid ferrofluid interface deformation and spray onset under electric and magnetic stresses," *Physics of Fluids* Vol. 29, No. 6, 2017, p. 064105.doi: 10.1063/1.4985141
7. Jackson, B. A., and King, L. B. "Time Resolved Divergence Mapping and Long Duration Emission Studies of an Ionic Liquid Ferrofluid Electrospray Source," *35th International Electric Propulsion Conference*. 2017.

8. Lozano, P., and Martinez-Sanchez, M. "Efficiency estimation of EMI-BF4 ionic liquid electrospray thrusters," *41st AIAA/ASME/SAE/ASEE Joint Propulsion Conference & Exhibit*. 2005, p. 4388.
9. Hawket, B., and Sabouri, H. "Saturatization Magnetization for ILFF Samples." 9/21/16, 2016.
10. Jain, N., Zhang, X., Hawkett, B. S., and Warr, G. G. "Stable and water-tolerant ionic liquid ferrofluids," *ACS Applied Materials & Interfaces* Vol. 3, No. 3, 2011, pp. 662-667.
11. Terhune, K. J., King, L. B., Prince, B. D., Jain, N., and Hawkett, B. S. "The effects of magnetic surface stress on electrospray of an ionic liquid ferrofluid," *52nd AIAA/SAE/ASEE Joint Propulsion Conference*. 2016, p. 4549.
12. Chiu, Y.-H., Gaeta, G., Levandier, D., Dressler, R., and Boatz, J. "Vacuum electrospray ionization study of the ionic liquid,[Emim][Im]," *International Journal of Mass Spectrometry* Vol. 265, No. 2, 2007, pp. 146-158.
13. Krejci, D., Mier-Hicks, F., Thomas, R., Haag, T., and Lozano, P. "Emission Characteristics of Passively Fed Electrospray Microthrusters with Propellant Reservoirs," *Journal of Spacecraft and Rockets*, 2017, pp. 1-12.doi: 10.2514/1.A33531
14. Gamero-Castaño, M. "Characterization of the electrosprays of 1-ethyl-3-methylimidazolium bis (trifluoromethylsulfonyl) imide in vacuum," *Physics of Fluids (1994-present)* Vol. 20, No. 3, 2008, p. 032103.
15. Gamero-Castano, M. "The structure of electrospray beams in vacuum," *Journal of Fluid Mechanics* Vol. 604, 2008, pp. 339-368.
16. Jackson, B. "Meniscus Modeling and Emission Studies of an Ionic Liquid Ferrofluid Electrospray Source Emitting from a Magneto-Electric Instability," 2018.
17. Terhune, K. J. "Influence of Magnetic Nanoparticles and Magnetic Stress on an Ionic Liquid Electrospray Source," 2017.